La Metallurgia Italiana
International Journal of the Italian Association for Metallurgy

AlSi10Mg alloy produced by Selective Laser Melting: relationships between Vickers microhardness, Rockwell hardness and mechanical properties

E. Cerri, E. Ghio

Selective Laser Melted Al10SiMg samples were directly aged at different temperatures and times to establish the best mechanical properties for this alloy. The problem of finding meaningful relationships between hardness and tensile strengths has been addressed for materials produced by additive manufacturing technology.
Relationships between hardness and yield and ultimate tensile strengths have been calculated by combining Hollomon parameters (the strain hardening exponent 'n' and the strength coefficient 'K') for the Selective Laser Melted AlSi10Mg alloy. Firstly, the pre-existing relationships were considered and verified for AlSi10Mg SLMed alloy. Moreover, the relationship derived from ASTM standards and Hollomon parameters were calculated from the engineering stress – strain curves. Afterwards, the measured values of Rockwell hardness (HRF) and Vickers hardness (HV) were related to each other by a simple equation according to theory. The results showed the accuracy of this equation with respect to the theoretical one. Finally, the yield strength, UTS and ultimate strength (σ_b, in function of strain hardening exponent and natural base e) obtained by different condition of thermal treatments (175 °C, 200 °C and 225 °C for 2h, 4h and 6h) were related to Vickers hardness values.

KEYWORDS: VICKERS HARDNESS, ROCKWELL HARDNESS, SELECTIVE LASER MELTING, ALSI10MG, YIELD STRENGTH, ULTIMATE TENSILE STRENGTH.

INTRODUCTION

Hardness and microhardness testing are fast and effective methods to determine the mechanical properties of metallic materials. In fact, they can be used and subsequently combined to have a first evaluation of mechanical properties such as yield and ultimate strength [1], playing an important role in the characterisation of new alloys and production process. In this context, the "quasi-non-destructive" test as reported by J.T. Busby et al. [1] has to be considered too.
At present, Additive Manufacturing (AM) (as Selective Laser Melting (SLM)) is one of the prevalent technologies for metallic component production, but mechanical properties of those parts should be optimized [2-4] during post-process heat treatments. As the research of new thermal treatments to optimise mechanical properties requires a large quantity of material, the use of suitable correlations and equations starting from hardness measurements could solve the pro-

Emanuela Cerri, Emanuele Ghio
D.I.A. University of Parma, Via G. Usberti 181/A, Parma, Italy
emanuela.cerri@unipr.it; emanuele.ghio@unipr.it

blem of optimization. In fact, the microstructure of SLMed components is thermodynamically unstable depending on temperature. Therefore, there is a great variation of yield strength, ultimate strength and elongation as function of treatment temperature and time duration [2, 5-7].
Within this framework, the proposal of a new simple correlation between Vickers microhardness and Rockwell hardness, and the verification of pre-existing equations confirmed only for the traditional as-cast state are the objectives of this study [8]. As reported by H. Chen et al. [9], the conversion equations for hardness depend on yield strength (σ_y), Young's modulus (E), hardening exponent (n), strain coefficient (K) and different coefficients related to hardness test as indenter geometry (φ_1, φ_2, φ_3 and φ_4) and load (F_t and F_0). Eq. (1) reports the correlation between Vickers microhardness and Rockwell hardness as studied by [9]:

$$HV = \frac{\varphi_1 \varphi_2^n \left(F_t^{1/m} - F_0^{1/m}\right)}{\left(\varphi_3 \varphi_4^n (1+m)\right)^{1/m} (k - HR)} \left(\frac{\left(E/\sigma_y\right)^n \sigma_y}{1+n}\right)^{1-1/m} \quad 1)$$

$$\begin{cases} \varphi_1 = \dfrac{2\eta\gamma_1 D_R \sin\left(\theta/2\right)}{S} \\ \varphi_2 = \gamma_2 \\ \varphi_3 = \alpha_1 D_R^2 \\ \varphi_4 = \alpha_3 \\ m = n\alpha_4 + \alpha_2 \end{cases} \quad 2)$$

where m is the loading exponent, α_1, α_2, α_3, α_4 are constants as reported by [9] and shown in Table 1, D_R is the diameter of ball Rockwell indenter, γ_1 and γ_2 are coefficients reported in Eq. (3).

$$\begin{cases} \gamma_1 = \dfrac{3\alpha_1}{8\tan^2\left(\theta/2\right)} = 1.986 \\ \gamma_2 = 0.05753 \end{cases} \quad 3)$$

Table 1 also reports the angle θ of the Vickers indenter, the known constants η, S and k, the load and pre-load force induced by Rockwell hardness test.

Tab.1 - Parameters used in the Eq. (1) for hardness conversion [9].

Vickers microhardness		Rockwell hardness (HRF)	
α_1	32.45	α_1	8.142
α_2	2	α_2	1.104
α_3	0.05753	α_3	0.1578
α_4	0	α_4	0.4333
θ	136°	k	130 (for F scale)
η	0.102		
S	0.002		

Furthermore, the relationship between hardness and tensile strength and the equation of tensile strength (σ_b) are as follows [9,10]:

$$HV = \frac{2\eta\gamma_1\left(e\gamma_2/n\right)^n \sigma_b \sin\frac{\theta}{2}}{1+n} \quad 4)$$

$$\sigma_b = K\left(\frac{n}{e}\right)^n \quad 5)$$

where e is the Nepero's number and n and K are the Hollomon parameters as reported by Table 2.

Tab.2 - Mechanical properties of AlSi10Mg dog-bone specimens obtained by tensile test (crosshead velocity: 0.02 mm/sec)

Temperature [°C]	HV	E [GPa]	σ_y [MPa]	UTS [MPa]	n	K [MPa]
T_as-built	112 ± 3	67 ± 3	215 ± 8	377 ± 14	0.255 ± 0.001	814 ± 1
B_as-built	122 ± 3	75 ± 5	297 ± 10	442 ± 15	0.204 ± 0.001	840 ± 1
T_175_2h	102 ± 2	74 ± 5	229 ± 8	363 ± 12	0.211 ± 0.001	712 ± 1
B_175_2h	122 ± 1	73 ± 5	241 ± 8	373 ± 12	0.201 ± 0.001	709 ± 1
T_175_4h	101 ± 2	73 ± 3	238 ± 6	375 ± 9	0.219 ± 0.001	754 ± 2
B_175_4h	115 ± 4	70 ± 5	252 ± 7	387 ± 11	0.213 ± 0.001	773 ± 2
T_175_6h	100 ± 3	73 ± 5	232 ± 9	370 ± 14	0.219 ± 0.001	748 ± 2
B_175_6h	113 ± 3	73 ± 3	285 ± 8	392 ± 11	0.200 ± 0.001	746 ± 2
T_200_2h	103 ± 3	72 ± 5	197 ± 5	327 ± 9	0.218 ± 0.001	741 ± 1
B_200_2h	110 ± 3	73 ± 5	238 ± 8	360 ± 13	0.193 ± 0.001	671 ± 1
T_200_4h	101 ± 3	71 ± 2	216 ± 6	351 ± 10	0.236 ± 0.001	749 ± 2
B_200_4h	109 ± 3	80 ± 5	232 ± 5	372 ± 12	0.228 ± 0.001	784 ± 2
T_200_6h	100 ± 1	75 ± 5	220 ± 5	353 ± 8	0.204 ± 0.001	701 ± 1
B_200_6h	102 ± 2	74 ± 5	235 ± 8	323 ± 8	0.211 ± 0.001	631 ± 1
T_225_2h	107 ± 3	75 ± 4	198 ± 5	323 ± 8	0.209 ± 0.001	631 ± 1
B_225_2h	110 ± 3	73 ± 5	217 ± 6	340 ± 9	0.202 ± 0.001	652 ± 1
T_225_4h	101 ± 3	76 ± 5	192 ± 6	313 ± 9	0.209 ± 0.001	609 ± 1
B_225_4h	105 ± 2	72 ± 5	207 ± 7	323 ± 11	0.194 ± 0.001	601 ± 1
T_225_6h	98 ± 3	75 ± 5	184 ± 6	300 ± 9	0.198 ± 0.001	562 ± 1
B_225_6h	102 ± 2	73 ± 4	199 ± 6	313 ± 9	0.196 ± 0.001	589 ± 1

A very simple relationship is reported by J.T. Busby et al. [1] where the yield strength linearly depends on HV microhardness (σ_y=3.55 HV). On the other hand, D. Tabor [11] and J. R. Cahoon [12] report other relationship between Vickers hardness and tensile strength, as follows:

$$UTS = \left(\frac{HV}{C}\right)(1-n)\left(\frac{12.5n}{1-n}\right)^{n} \quad 6)$$

$$\sigma_y = \left(\frac{HV}{3}\right)\left(\frac{1}{10}\right)^{n} \quad 7)$$

$$UTS = \frac{HV}{2.9}\left(\frac{n}{0.219}\right)^{n} \quad 8)$$

where HV is the Vickers hardness, C is a value between 2.9 and 3 as suggested by D. Tabor, n is the strain hardening and can be changed in Meyer's exponent as reported by [11,12]. J.R. Cahoon [12] suggested the range from 2.9 to 3.1 for the constant C. Finally, it is necessary to emphasize that the units of UTS and σ_y can be converted from kgf/mm^2 to MPa.

In this context, it is possible to observe that several studies and correlations are focused on steels such as AISI 304 [13], AISI 1020, AISI 316L [14] and on aluminium alloys like AA 6063-T5 and AA 1350 [14]. At present, no results are reported for AlSi10Mg produced by SLM. Therefore, this study aims to calculate and verify the correlations between the mentioned properties.

MATERIAL AND METHODS

Bulk specimens of AlSi10Mg aluminium alloy were produced by SLM from spherical gas-atomized powder with nominal composition shown in Table 3. SLM processing was carried out on a platform heated at 150°C using an SLM500 device (SLM Solutions) equipped with an Yb-YAG laser. The parameters used for preparing the samples are as follows: scanning speed 1550 mm/s, power 350 W, layer thickness 50 µm, hatch spacing 17 µm. High purity argon gas was used during SLM processing in order to avoid oxygen contamination.

Tab.3 - Chemical composition of AlSi10Mg.

Al [%]	Si [%]	Fe [%]	Mg [%]	Cu [%]	Mn [%]	Zn [%]	Ti [%]	Pb [%]	Sn [%]
Bal.	9.60	0.10	0.38	< 0.05	< 0.01	<0 .01	< 0.01	< 0.01	< 0.01

Solid geometries of 25 merged cylindrical bars with total length of 100 mm, total height of 300 mm and diameter of 10 mm were built. At the same time, bars with a 10x10 mm^2 area section were built in the same job with the same final height. Afterwards, tensile samples were cut and machined according to ASTM E804 from the solid geometries.

Specimens were heat treated at 175°, 200° and 225°C for 2, 4 and 6h in an electric muffle-furnace. The same conditions were used for samples obtained by the billet.

Tensile tests were performed at room temperature using a MTS810 machine in according to ASTM E8 standard, at a strain rate of 0,008 s^{-1} on as-built and heat treated specimens.

Vickers microhardness (HV) was measured with a load of 500 g and a dwell time of 15s according to UNI EN ISO 6507. The average HV values measured on dog bone samples have been related to their tensile properties (engineering stress strain curves).

Rockwell hardness was measured, in according to UNI EN ISO 6508, with 10 kgf of pre-load and 60 kgf of load and ball indenter D_R of 1.588 mm diameter (HRF). HRF was evaluated on samples (nominated BS in this paper) cut from the bar.

Mathematical correlations were calculated by OriginPro 9.0 and the results compared to Eqs. (1) and (2).

The analysis of engineering stress – strain curves obtained from tensile samples determined the calculation of Hollomon's parameters. In this case, the correlations have been evaluated according to Eqs. (4), (5), (6) and (13).

RESULTS AND DISCUSSION

Relationship between HV and HRF

In this section, Vickers microhardness HV values and Rockwell HRF values are considered to determine the relationship between these two different hardness scales. All results obtained by hardness tests, performed on as-built 'BS' and on thermal treated 'BS' samples, are reported in Fig. 1. Fig. 1 shows the trends that correlate HV microhardness to HRF hardness according to Eq. (1). In details, these plots were drawn considering data results from tensile tests (Table 2), the Eq. (2), the parameters reported in Table 1 and the HRF values between 60 and 105. It is possible to observe that the upper and lower curves of Fig. 1 belong to the B_as-built state and T_225_6h, respectively. They create a domain for the included area where all the other heat treatment conditions are placed in. This region will be fundamental for comparison with test results. The aging at 225 °C for 6h is the thermal treatment that induces the most significant decrease in hardness compared to the other heat treatments reported in Table 2.

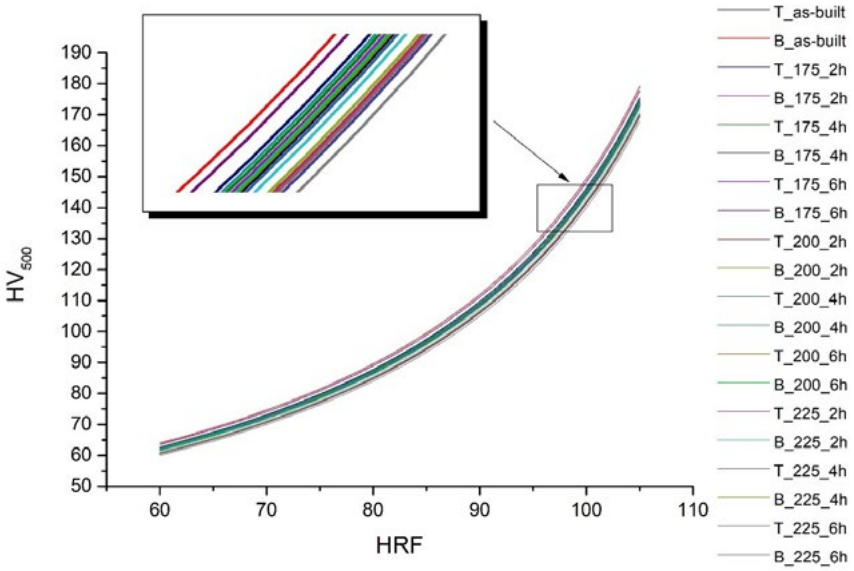

Fig.1 - Curves obtained by Eq. (1) and parameters reported in Table 2.

It should be noted that the Hollomon's parameters (Table 2), obtained plotting the true stress – strain curves in a Log-Log diagram as reported by [11, 16-18], are also confirmed by I. Rosenthal et al. [3] working at the same heat treatment conditions and by [4,19]. As reported by P.A. Rometsch et al. [20], the strain hardening values of heat-treated aluminium casting alloys are much lower than those given in Table 2. This variation is attributable to the different microstructure between as-cast case and as-built case for AlSi10Mg alloy or heat treated with non-conventional treatments. In fact, as reported in Fig. 2a, [3] the size and morphology of microstructure and Si particles are greater than those reported in Fig. 2b. As widely discussed in literature, the particular shapes and distribution of Si eu-

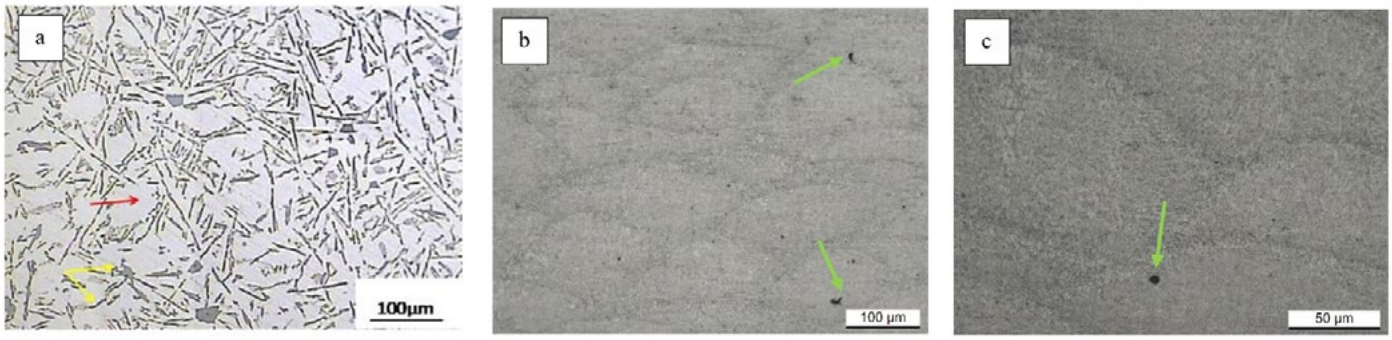

Fig.2 - Fig. 2 - OM images of (a) as-cast AlSi10Mg [3], (b) as-built AlSi10Mg SLMed (200x) and (c) as-built AlSi10Mg SLMed (500x). Red and yellow arrows mark Al matrix and Si eutectic, green arrows mark porosity.

tectic and precipitates induce high mechanical properties and consequently high Hollomon's parameters in the as-built cases and in non-conventional thermal treatment cases [2-7].

In general, the range of strain hardening exponent values suggests that the material could show a large uniform elongation. If there was a premature fracture, this would be due to the presence of defects within the microstructure [21]. Finally, in Fig. 3 the true stress – strain curves and the trends of Hollomon's law ($\sigma = K\varepsilon^n$,[9]) are illustrated. All trends are comparable to those reported by [9].

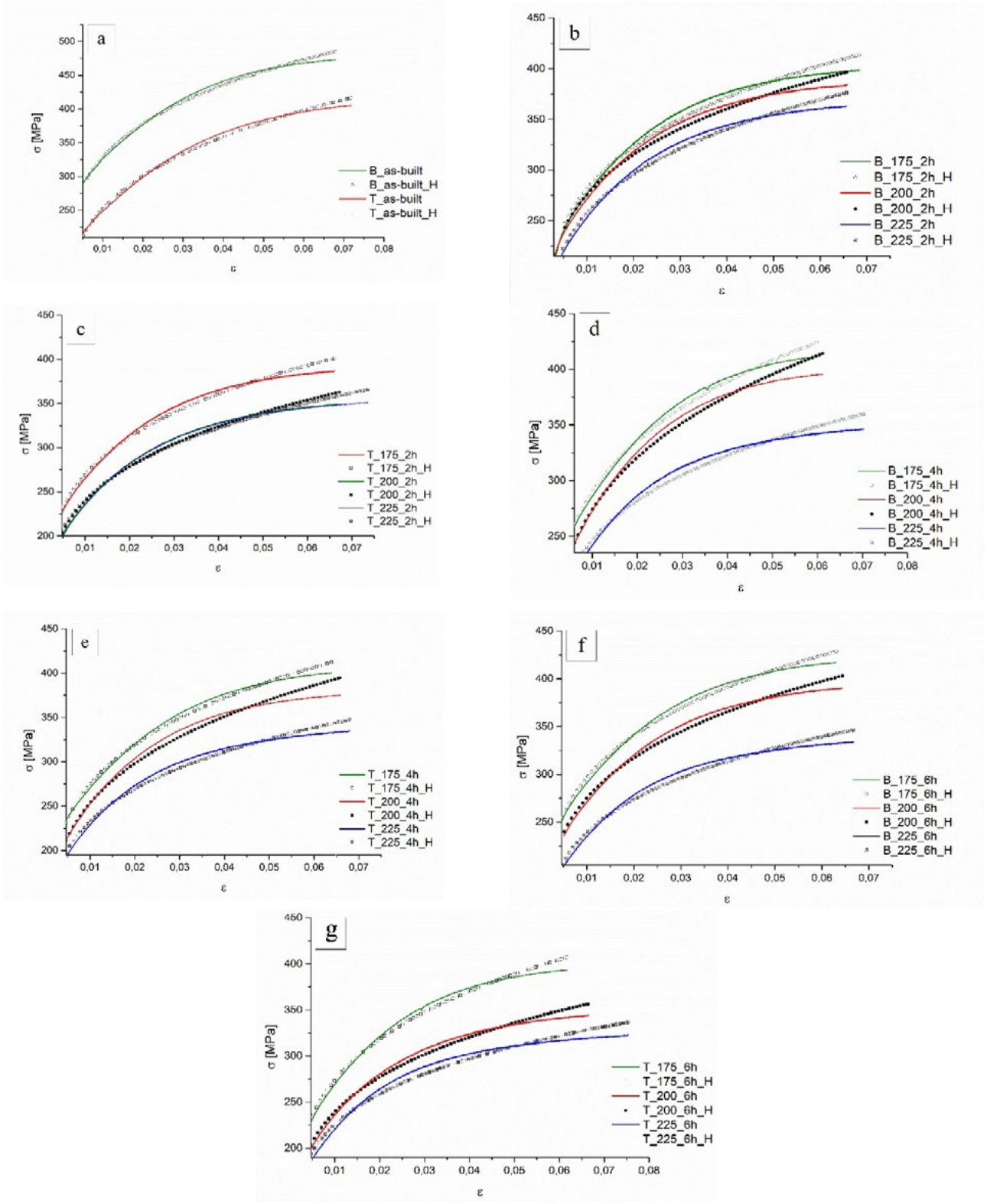

Fig.3 - True stress - strain curves and Hollomon's law for different heat treatment conditions: (a) as-built, (b) and (c) 2h at 175, 200 and 225 °C, (d) and (e) 4h at 175, 200 and 225 °C, (f) and (g) 6h at 175, 200 and 225 °C.

Fig. 4 shows all the results obtained by hardness tests performed on as-built and on aged samples. Moreover, in the same Figure, the linear fit (green) and the polynomial fit (orange) are calculated in Eqs. (9) and (10) respectively:

$$HV_{500}=1.7596\ HRF-48.9727 \quad (9)$$

$$HV_{500} = 0.0284\ HRF^2 - 2.8195\ HRF + 132.4074 \quad (10)$$

The coefficients of determination (R^2) are 0.945 and 0.963 for Eq. (9) and Eq. (10), respectively.

In Fig. 5, the overlap of Fig. 4 and the domain of existence previously mentioned (upper and lower curve in Fig. 1) are reported. It is possible to observe that comparing the linear and polynomial fit to domain derived from Eq. (1), the Eq. (10) correlates the two hardness scales with a better approximation than the Eq. (9). In other words, the polynomial function (orange line) has a greater range of existence contained within the domain (Fig. 1) than the linear function (green function). Furthermore, both solutions have an intrinsic dependence on tensile properties as yield strength and Young's modulo due to their good approximation to Eq. (1).

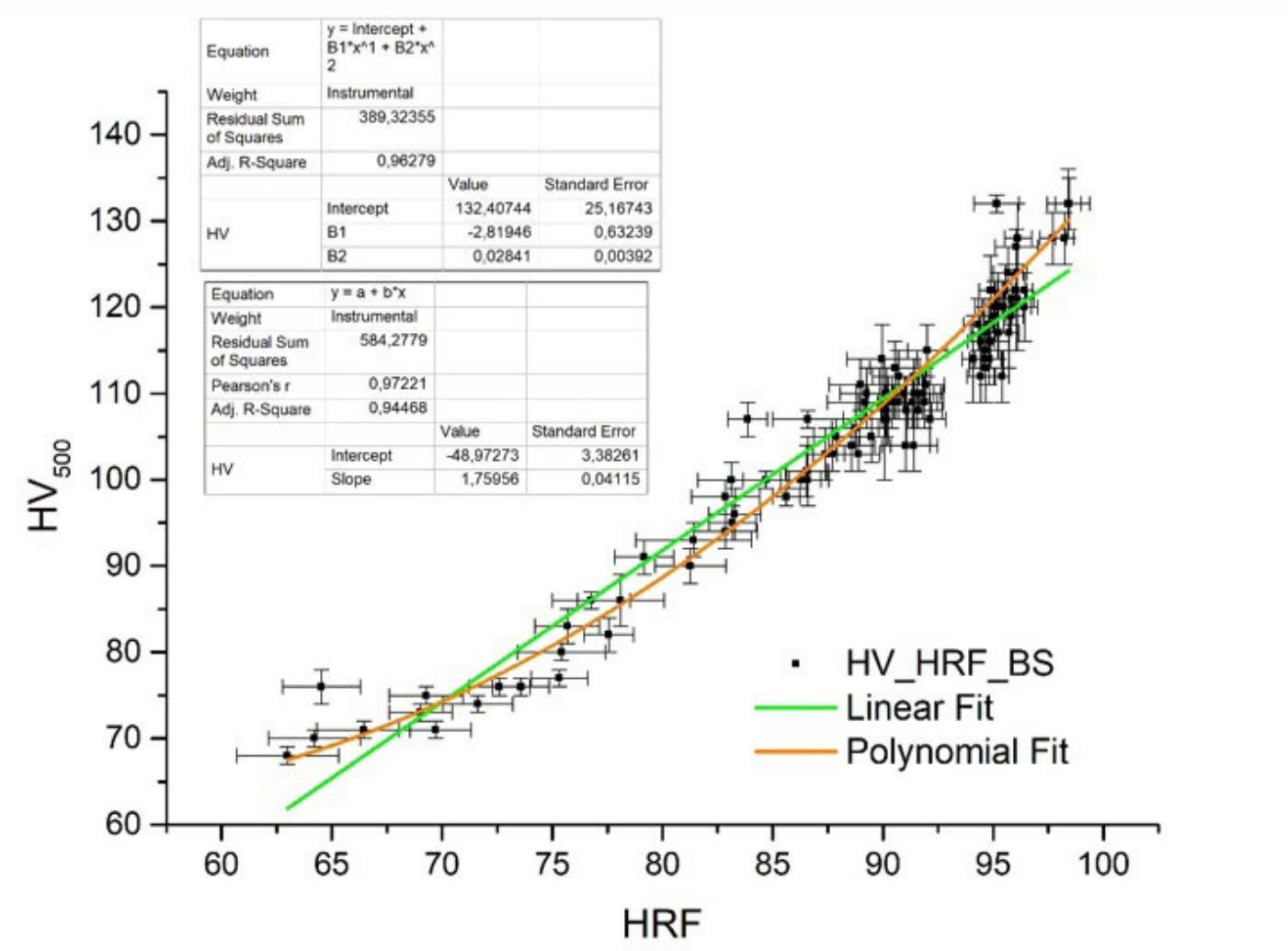

Fig.4 - Vickers microhardness and Rockwell hardness values of as-built BS and thermal treated BS.

In the same scenario, the equations described above make it possible to simplify the problem of

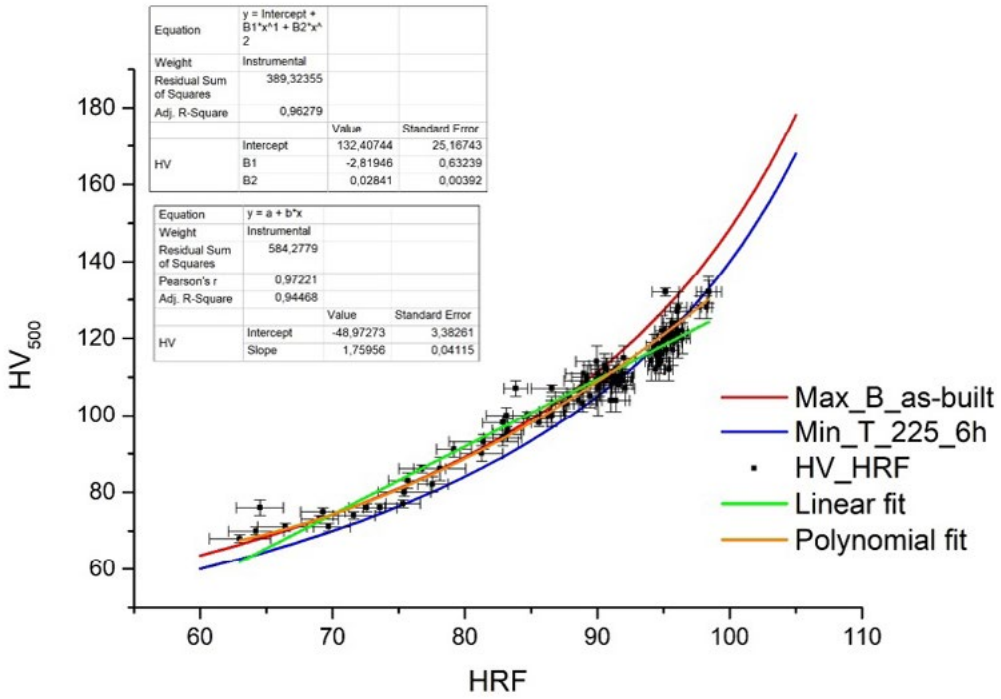

Fig.5 - Overlap between the min and max curve obtained by Eq. (1) (red and blu curves) and the correlation reported by Eqs. (9) and (10).

correlation between hardness scales. In other words, HV microhardness and HRF hardness can be related by a polynomial fit equation without the necessary determination of mechanical properties of considered samples. This is also confirmed by the fact that R^2 has an excellent value for Eq. (10).

Relationships between strength and hardness

In this section, the focal point is the correlation of yield strength to HV and the dependence of UTS on HV (Figs. 6 and 7, respectively). Many correlations found in literature depend on the strain hardening (n) and on various multiplication coefficients [9-12]; furthermore, it would be possible to list other simpler equations where hardness and tensile strengths have a direct proportionality [1,18].

Figs. 6 and 7 report the average value distributions obtained by microhardness and tensile tests. In addition, the red lines represent the linear fit between UTS and HV and between yield strength and HV as expressed in Eq. (11) and Eq. (12) respectively.

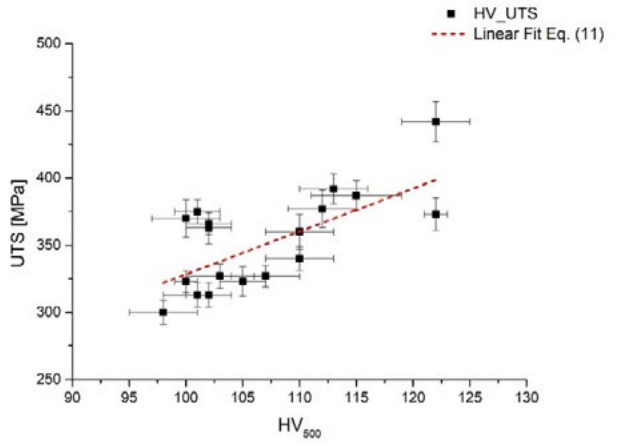

Fig.6 - Linear fit between HV microhardness and UTS values reported in Table 2.

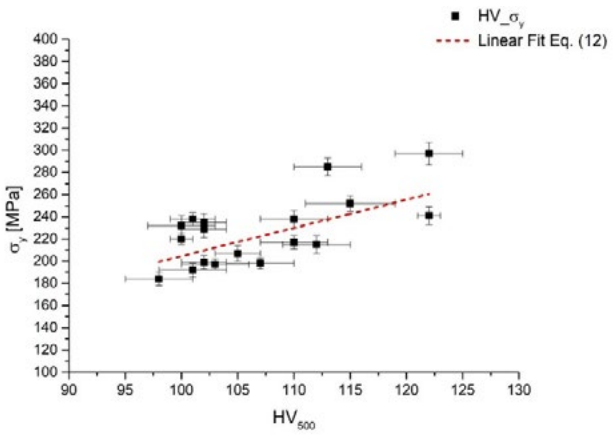

Fig.7 - Linear fit between HV microhardness and σ_y values reported in Table 2.

$$UTS=3.20\ HV_{500}+8.58 \quad (11)$$

$$\sigma_y=2.54\ HV_{500}-49.62 \quad (12)$$

So, looking at the Eq. (4) and comparing it to Eq. (11) subsequently, it is necessary to consider Eqs. (3) and (5) and the parameters reported in Tables 1 and 2. At this point it is possible to determine HV as function of σ_b [9, 10] as predicted in Eq. (3). As reported by Li et al. [10], the σ_b is the maximum strength obtained in the engineering stress – strain curve. In other words, this strength is comparable to the UTS.

Tab.4 - Results of HV and tensile strength obtained by Eq. (4) and Eq. (5) and real values.

Temperature [°C]	HV, [9]	HV	Error [%]	σ_b [MPa], [10]	UTS [MPa]	Error [%]
T_as-built	118	112 ± 3	5	445	377 ± 14	15
B_as-built	146	122 ± 3	17	495	442 ± 15	11
T_175_2h	121	102 ± 2	16	415	363 ± 12	13
B_175_2h	125	122 ± 1	2	420	373 ± 12	11
T_175_4h	124	101 ± 2	19	434	375 ± 9	13
B_175_4h	130	115 ± 4	12	449	387 ± 11	14
T_175_6h	124	100 ± 3	19	431	370 ± 14	14
B_175_6h	132	113 ± 3	14	442	392 ± 11	11
T_200_2h	123	103 ± 3	16	428	327 ± 9	15
B_200_2h	122	110 ± 3	10	403	360 ± 13	11
T_200_4h	116	101 ± 3	11	421	351 ± 6	16
B_200_4h	130	109 ± 3	16	445	372 ± 8	16
T_200_6h	121	100 ± 1	18	368	353 ± 8	12
B_200_6h	109	102 ± 2	6	417	323 ± 8	12
T_225_2h	113	107 ± 3	5	369	323 ± 8	11
B_225_2h	106	110 ± 3	4	386	340 ± 9	12
T_225_4h	105	101 ± 3	4	356	313 ± 9	12
B_225_4h	101	105 ± 2	4	361	323 ± 11	10
T_225_6h	105	98 ± 3	7	335	300 ± 9	10
B_225_6h	106	102 ± 2	4	332	313 ± 9	11

With these premises, Table 4 shows HV and σ_b values calculated through Eqs. (3), (4) and (5) respectively; it also reports the percentage errors calculated by comparing these values to HV and UTS as measured by microhardness and tensile tests. In the case of HV, an overestimation of 19% and an underestimation of 4% are obtained comparing the values with HV, [9]. These error values are comparable to those reported by J.Y. Kim et al. [22] and they depend on all strength values, σ_b, calculated by Eq. (5). In fact, as reported in Table 4, the lower error of 10% confir-

ms the high overestimation of single HV hardness values (Fig. 8). As reported, it is useful remember that HV reported in Eq. (4) depends on σ_b. By considering the values of HV and UTS reported in the same Table, and for the fact that σ_b is the UTS [10], it is possible to compare the linear fit (red line, Eq. (11)) of these values with the maximum and minimum of Eq. (4) in Fig. 8. These curves, cyan and blue respectively, are calculated as expressed above and with the same method used in Fig. 1. So, as already assessed in Table 4 and shown in Fig. 8, the max and min curve are shifted upwards compared to linear fit (Eq. (11)). This can be attributed to the percentage errors related to σ_b once again.

As the aim of this paper is the determination of a simple correlation between HV and UTS, it is opportune to start from the omission of σ_b. In fact, the use of UTS in the Eq. (6) and Eq. (8) leads to account for a lower overestimation of HV values than the use of the Eq. (4). In fact, this value decrease from 12% to 9%. Fig. 9 shows the trends of Tabor and Cahoon equations compared to linear fit (Eq. (11)) shown in Fig. 6. It is possible to observe that the slopes are fully comparable (3.55 for Eq. (6)

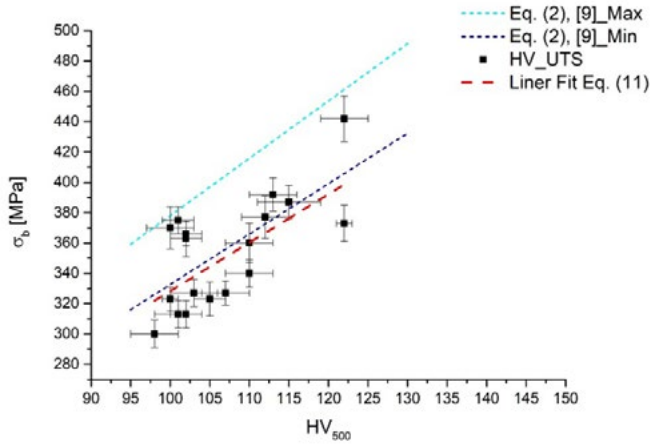

Fig.8 - Correlation between Tabor (Eq. (6)) and Cahoon equation (Eq. (8)) and the linear fit reported in Fig. 6.

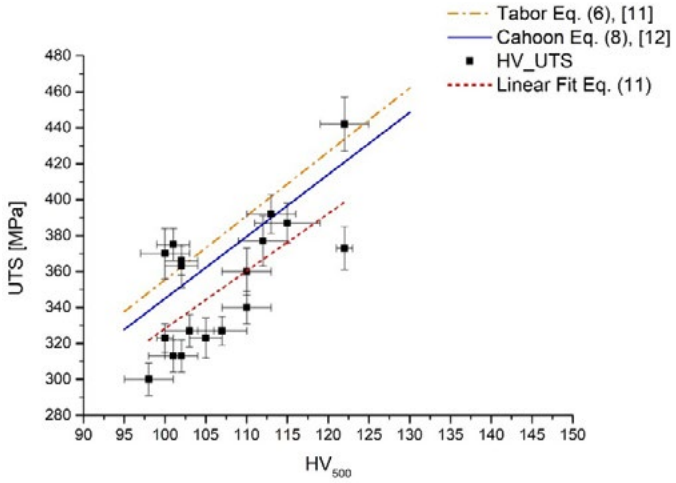

Fig.9 - Results obtained by Eq. (2) (cyan line for the max and blue line for the min) and by linear interpolation reported in Fig. 6.

and 3.45 for Eq. (6)), but using the Cahoon equation rather than the Tabor one it is possible to get a better approximation of Eq. (11). For the reasons expressed and remembering the Tabor equation, the factor C calculated for AlSi10Mg SLMed is exactly 2.99. As reported by J. R. Cahoon [12], the suggested range value of C is from 2.9 to 3.1.

As regards the correlation between Vickers microhardness and yield strength, the considered equations are reported in Fig. 10. All reported values of HV and σ_y are related through the following linear fit:

$$\sigma_y = 2.54\ HV_{500} - 49.62 \qquad 12)$$

The standard error associated to the slope is 0.860. In this case, the best fit for aluminium alloys is represented by the Petty equation [17]:

$$\sigma_y = 0.148\ HV - 1.59 \qquad 13)$$

It should be noted that the unit of measure of yield strength is in ton/in^2, so the conversion in MPa must be done multiplying for 15.4448. By applying this conversion factor, the slope of Petty equation is close to the slope reported in Eq. (12). In addition, the similar trend between this last equation and Eq. (13) leads to suppose that the SLM process does not change the existing relationship between HV and the yield strength.

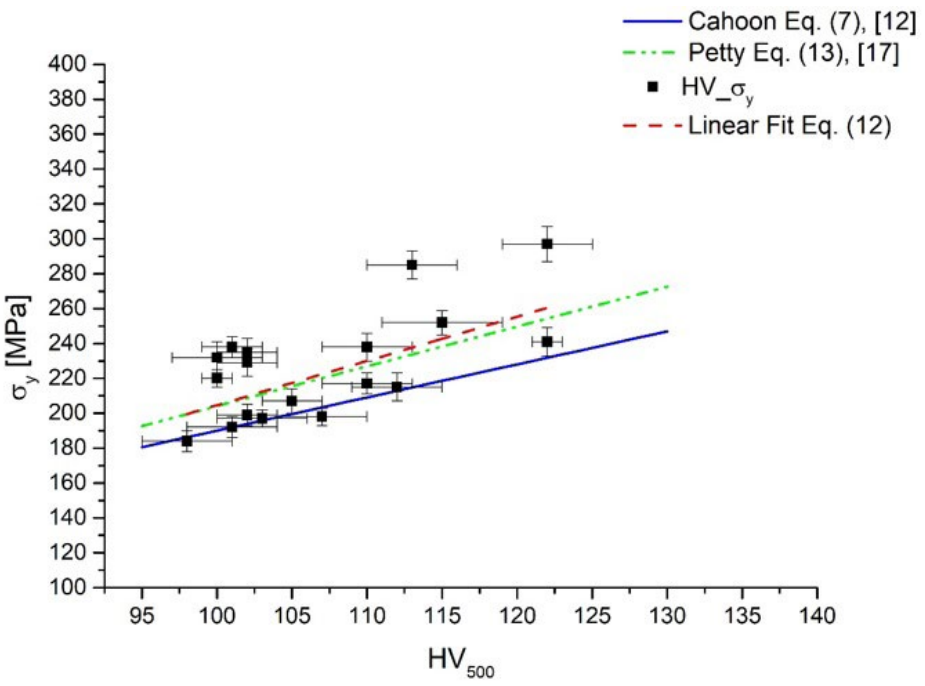

Fig.10 - Correlation between microhardness and yield strength derived by Cahoon (Eq. (7)) and Petty equation (Eq. (13)) and linear fit reported in Fig. 7.

On the contrary, Eq. (7) underestimates the yield strength. So, the Eq. (14) introduces the coefficient ξ to better approximate the Cahoon equation to this study, as also performed by J.S. Keist et al. [23]. The value of ξ was estimated to be 0.891, average value of all cases reported in Table 2.

$$\sigma_y = \left(\frac{HV}{\xi \cdot 3}\right)\left(\frac{1}{10}\right)^n \qquad 14)$$

Finally, as reported by S.C. Krishna et al. [18], it is possible to compare the linear fit with the ratio between UTS and yield strength: i) Low ratio (U-y < 1.20), ii) Medium ratio (1.20 < U-y < 1.52) and iii) High ratio (U-y > 1.52). In the present study, the average of all calculated ratios is 1.57. The results reported in Table 5 show similar proportionality coefficient between present results and their correlations.

It should be noted the proportionality coefficient can be compared if the linear interpolations have the coordinate zero as intercept. From this premise, the points reported in Figs. 5 and 6 are correlated with Eqs. (15) and (16) shown in Table 5; equations calculated with the same metod used for Eqs. (11), (12).

Tab.5 - Equations (15) and (16) obtained by linear fit and reported by [20].

Data type	Equations	R^2	Valid range (HV)	Reference
High U-y ratio	UTS=3.865 HV	0.845	50 – 142	S.C. Krishna et al. [20]
	σ_y=1.97 HV	0.665		
	UTS=3.328 HV	0.995	95 – 125	Eq. (15)
	σ_y=2.155 HV	0.987		Eq. (16)

CONCLUSIONS

In the present paper, the relationships between HV and HRF hardness and HV and tensile strengths have been studied for AlSi10Mg alloy processed by SLM. Correlations were found for samples in the as built conditions and after aging treatments. The main conclusions can be summarised as follows:

- The relationship between Vickers microhardness (HV) and Rockwell hardness (HRF) can be approximated by a second order equation. The dependence on mechanical properties and on geometry parameters of hardness tests are intrinsically expressed.
- A linear relationship between Vickers microhardness and tensile properties can be applied with good approximation. The minimum overestimation of UTS values is obtained by Cahoon equation. For yield strength, the best approximation is obtained by Petty equation.
- For this alloy the factor C considered in Tabor equation was calculated; the value obtained is 2.99.
- The ranges suggest for strain hardening n is from 0.19 to 0.25 and for strength coefficient K is from 589 to 890 MPa for the case reported in this paper.

REFERENCES

[1] J. T. Busby, M. C. Hash, G. S. Was, The relationship between hardness and yield stress in irradiated austenitic and ferritic steels, Elsevier, Jou. of Nuclear Materials, 336 (2005) 267 – 278. https://doi.org/10.1016/j.jnucmat.2004.09.024

[2] N. T. Aboulkhair, I. Maskery, C. Tuck, I. Ashcroft, N. M. Everitt, The microstructure and mechanical properties of selective laser melted AlSi10Mg: The effect of a conventional T6-like heat treatment, Elsevier, Mat. Sci. Eng., 667 (2016) 139 – 146. https://dx.doi.org/10.1016/j.msea2016.01.092

[3] I. Rosenthal, A. Stern, N. Frage, Strain rate sensitivity and fracture mechanism of AlSi10Mg parts produced by Selective Laser Melting, Elsevier, Mat. Sci. Eng., 682 (2017) 509 – 517. https://dx.doi.org/10.1016/j.msea.2016.11.070

[4] B. Chen, S.K. Moon, X. Yao, G. Bi, J. Shen, J. Umeda, K. Kondoh, Strenght and strain hardening of a selective laser melted AlSi10Mg alloy, Elsevier, Scripta Mat., 141 (2017) 45 – 49. https://doi.org/10.1016/j.scriptamat.2017.07.025

[5] W. Li, S. Li, J. Liu, A. Zhang, Y. Zhou, Q. Wei, C. Yan, Y. Shi, Effect of heat treatment on AlSi10Mg alloy fabricated by selective laser melting: Microstructure evolution, mechanical properties and fracture mechanism, Elsevier, Mat. Sci. Eng., 63 (2016) 116 – 125. https://dx.doi.org/10.1016/j.msea.2016.03.088

[6] K. Kempen, L. Thijs, J. Van Humbeeck, J.P. Kruth, Mechanical properties of AlSi10Mg produced by Selective Laser Melting, Elsevier, SciVerse ScienceDirect, 39 (2012) 439 – 446. https://doi.org/10.1016/j.phpro.2012.10.059

[7] N. Read, W. Wang, K. Essa, M.M. Attallah, Selective laser melting of AlSi10Mg alloy: Process optimisation and mechanical properties development, Elsevier, 65 (2015) 417 – 424. https://dx.doi.org/10.1016/j.matdes.2014.09.044

[8] ASTM International E140-12bel, ASTM International, West Conshohocken, PA, 2013.

[9] H. Chen, L.X. Cai, Theoretical conversions of different hardness and tensile strength for ductile materials based on stress-strain curves, Metallurgical and Materials transactions A, 49A (2018) 1090 – 1101. https://doi.org/10.1007/s11661-018-4468-8

[10] J. Li, F. Li, X. Ma, Q. Wrang, J. Dong, Z. Yuan, A strain-dependent ductile damage model and its application in the derivation of fracture toughness by micro-indentation, Mat. And Des., 67 (2015) 623 – 630. https://dx.doi.org/10.1016/j.matdes.2014.11.010

[11] D. Tabor, The hardness of metals, Oxford, pp. 105 – 113, 1951.

[12] J.R. Cahoon, An improved equation relating hardness to ultimate strength, Met. Transactions, 3 (1972) 3040. https://doi.org/10.1007/BF02652880

[13] J. Moteff, R.K. Bhargava, W.L. WcCullough, Correlation of the hot-hardness with the tensile strength of 304 stainless steel to

temperatures of 1200 °C, Met. Trans., 6 (1975) 1101 – 1104. https://doi.org/10.1007/BF02661365

[14] G. Pintaude, A. Hoechele, G. Cipriano, Relation between strain hardening exponent of metals and residual profiles of deep spherical indentation, Mat. Sci. Tech., 28 (2012) 1051 – 1054. https://doi.org/10.1179/1743284711Y.0000000107

[15] ASTM International E8/E8M – 13a, Standard Test Methods for Tension Testing of Metallic Materials, PA, 2013.

[16] G.E. Dieter, Mechanical Metallurgy, 3rd ed., Mc Graw-Hill- New York, (1986) 243 – 248.

[17] A. Bhaduri, Mechanical Properties and Working of Metals and Alloys, Springer, 264 (2018) 46 – 49.

[18] S.C. Krishna, N.K. Gangwar, A.K. Jha, B. Pant, On the prediction of strength from hardness for copper alloys, Jou. of Mat., 2013 (2014) 6. https://dx.doi.org/10.1155/2013/352578

[19] L. Zhou, A. Mehta, E. Schulz, B. McWilliams, K. Cho, Y. Sohn, Microstructure, precipitates and hardness of selectively laser melted AlSi10Mg alloy before and after heat treatment, Mat. Characterization, 143 (2018) 5 – 17. https://doi.org/10.1016/j.matchar.2018.04.022

[20] P.A. Romescth, G.B. Schaffer, An age hardening model for Al-7Si-Mg casting alloys, Mat. Sci. & Eng. A, 325 (2002) 424 – 434. https://doi.org/10.1016/S0921-5093(01)01479-4

[21] P.K. Gokuldoss, Work hardening in selective laser melted Al-12Si alloy, Mat. Design Process Comm., Wiley, vol. 1, 2019. https://doi.org/10.1002/mdp2.46

[22] J.Y. Kim, K.W. Lee, J.S. Lee, D. Kwon, Determination of tensile properties by instrumented indentation technique: Representative stress and strain approach, ScienceDirect, 201 (2006) 4278 – 4283. https://doi.org/10.1016/j.surfcoat.2006.08.054

[23] J.S. Keist, T.A. Palmer, Development of strength-hardness relationships in additively manufactured titanium alloys, Mat. Sci. & Eng. A, 693 (2017) 241 – 224, 2017. https://dx.doi.org/10.1016/j.msea.2017.03.102